Caveolin-1 Increases Proinflammatory Chemoattractants and Blood–Retinal Barrier Breakdown but Decreases Leukocyte Recruitment in Inflammation

Xiaoman Li,[1,*] Xiaowu Gu,[1] Timothy M. Boyce,[1] Min Zheng,[1] Alaina M. Reagan,[1] Hui Qi,[1] Nawajes Mandal,[1] Alex W. Cohen,[1] Michelle C. Callegan,[1] Daniel J. J. Carr,[1,2] and Michael H. Elliott[1]

[1]Department of Ophthalmology/Dean McGee Eye Institute, University of Oklahoma Health Sciences Center, Oklahoma City, Oklahoma, United States
[2]Department of Microbiology & Immunology, University of Oklahoma Health Sciences Center, Oklahoma City, Oklahoma, United States

Correspondence: Michael H. Elliott, Department of Ophthalmology, University of Oklahoma Health Sciences Center, 608 Stanton L. Young Boulevard, Oklahoma City, OK 73104, USA;
michael-elliott@ouhsc.edu.

XL and XG contributed equally to the work presented here and should therefore be regarded as equivalent authors.

Current affiliation: *Key Laboratory of Medical Cell Biology, China Medical University, Shenyang, Liaoning Province, China.

Submitted: April 16, 2014
Accepted: August 12, 2014

Citation: Li X, Gu X, Boyce TM, et al. Caveolin-1 increases proinflammatory chemoattractants and blood–retinal barrier breakdown but decreases leukocyte recruitment in inflammation. *Invest Ophthalmol Vis Sci*. 2014;55:6224–6234. DOI:10.1167/iovs.14-14613

Purpose. Caveolin-1 (Cav-1), the signature protein of caveolae, modulates inflammatory responses, and innate immunity. However, Cav-1's role in retinal inflammation has not been rigorously tested. In this study, we examined the effect of Cav-1 ablation on the sensitivity of the retina to inflammation.

Methods. Cav-1 knockout (KO) mice were challenged by intravitreal injection of lipopolysaccharide (LPS) and inflammatory cell recruitment was assessed by flow cytometry and immunohistochemistry. Leukostasis was assessed in retinal flatmounts after perfusion with FITC-labeled Concanavalin A (FITC-ConA). Chemoattractants were measured by multiplex immunoassays. Blood–retinal barrier (BRB) breakdown was assessed quantitatively by a FITC-dextran permeability assay. The ratio of extravascular to total immune cells was determined by CD45 immunohistochemistry of retinal flatmounts.

Results. Inflammatory challenge resulted in significant blunting of proinflammatory cytokine (monocyte chemoattractant protein-1 [MCP-1/CCL2], CXCL1/KC, IL-6, and IL-1β) responses as well as reduced inflammatory BRB breakdown in Cav-1 KO retinas. Paradoxically, Cav-1 deficiency resulted in significantly increased recruitment of immune cells compared with controls as well as increased leukostasis. A similar ratio of extravascular/total leukocytes were found in Cav-1 KO and wild-type (WT) retinas suggesting that Cav-1 deficient leukocytes were as competent to extravasate as those from WT mice. We found increased levels of circulating immune cells in naïve (not challenged with LPS) Cav-1 KO mice compared with controls.

Conclusions. Caveolin-1 paradoxically modulates inflammatory signaling and leukocyte infiltration through distinct mechanisms. We hypothesize that Cav-1 expression may enhance inflammatory signaling while at the same time supporting the physical properties of the BRB.

Keywords: inflammation, blood–retinal barrier, caveolin, cytokines

The eye has evolved both structural and functional mechanisms that reduce inflammation to promote a clear ocular media anteriorly and to maintain retinal homeostasis posteriorly.[1,2] Structurally, the retina is physically separated from the immune system by two tight blood–retinal barriers (BRBs) provided by the RPE[3] and inner retinal vascular endothelium,[4] respectively. However, separation alone is not sufficient to maintain the relatively immunosuppressed retinal environment and the posterior segment has evolved mechanisms to actively reduce immune responses.[5–7] Failure to blunt inflammatory responses likely plays a critical role in the pathophysiology of many retinal degenerative and inflammatory conditions, notably AMD, glaucoma, diabetic retinopathy, and uveitis.[8–11] Thus, a clearer understanding of the mechanisms by which the retina responds to inflammatory insult is essential to designing novel therapies for retinal inflammatory disease.

Caveolin-1 (Cav-1) is the signature protein of caveolae membrane microdomains, and has been implicated in diverse, cell context-specific functions including endocytosis, lipid trafficking, signal transduction compartmentalization, and mechanosensation (See references 12 and 13 for review). In the retina, caveolae and/or Cav-1 are localized to several retinal cell types including Müller glia,[14–16] RPE,[17,18] retinal vascular endothelium,[19–22] mural cells,[23–26] and neurons,[27–31] and play important regulatory roles in BRB integrity and retinal homeostasis.[4,19,22,23,25,32–34] Cav-1 expression levels and caveolae numbers are dramatically increased in retinal inflammatory diseases such as uveitis and in animal models of diabetic retinopathy.[4,19,24,35] Caveolin-1 has recently been identified as a modulator of inflammatory responses in both innate and adaptive immunity.[36,37] A growing body of evidence implicates Cav-1 in the regulation of toll-like receptor (TLR) signaling although the literature is somewhat confounding as to whether

Cav-1 promotes[38–44] or suppresses[45–50] innate inflammatory responses.

Given our previous work showing that Cav-1 deficiency results in increased BRB permeability[23] and alterations in retinal ion homeostasis,[34] we hypothesized that loss of Cav-1 would promote inflammatory signaling in the retina. As Cav-1 can modulate TLR4 signaling outside of the eye[38,41,50] and Cav-1 expression is increased during ocular inflammation,[19,35] we examined the consequence of Cav-1 ablation on the inflammatory response induced by the intravitreal administration of the TLR4 ligand, lipopolysaccharide (LPS/endotoxin).[51] The results presented in this paper suggest that Cav-1 ablation reduces proinflammatory cytokine expression and inflammatory BRB breakdown in the retina, but paradoxically, results in increased immune cell influx. We postulate that the paradox between signaling and infiltration reflects a complex interplay between cell-specific differences in local inflammatory responses and from systemic immune dysfunction resulting from global Cav-1 deficiency. The profound effect on local inflammatory cytokine suppression suggests that Cav-1 could represent a novel therapeutic target to suppress local inflammatory responses.

Methods

Animals

Experiments were performed on Cav-1 knock-out (KO) mice C57BL/6J background (stock number 007083; The Jackson Laboratory, Bar Harbor, ME, USA) with C57BL/6J mice (stock number 000664; The Jackson Laboratory) used as wild-type (WT) controls.[23,34] Caveolin-1 KO mice were bred at the specific pathogen-free University of Oklahoma Health Sciences Center Rodent Barrier facility (Oklahoma City, OK, USA). Control mice purchased from The Jackson Laboratory and KO mice were transferred to the biocontainment caging in the conventional vivarium at the Dean A. McGee Eye Institute (University of Oklahoma Health Sciences Center, Oklahoma City, OK, USA) and maintained for a 2-week acclimatization period prior to experimentation. Breeding and stock mice from our colony were screened for the *rd8* mutation and all mice ($n = 33$) were negative. All procedures were approved by the Institutional Animal Care and Use Committee of the University of Oklahoma Health Sciences Center and were carried out in accordance with the ARVO Statement for the Use of Animals in Ophthalmic and Vision Research.

Endotoxin-Induced Uveitis Model

Ocular inflammation was induced by intravitreal injection of 0.5 or 1 μg LPS (*Salmonella typhimurium;* Sigma-Aldrich Corp., St. Louis, MO, USA) in 1 μL of sterile PBS as described[51] with slight modification. Mice anesthetized by intraperitoneal injection of ketamine (80 mg/kg)/xylazine (5 mg/kg) and topical 0.5% proparacaine were intravitreally injected with LPS in one eye and PBS vehicle in the contralateral eye using borosilicate glass micropipettes (Kimble Glass, Inc., Vineland, NJ, USA) beveled to a bore size of 10 to 20 μm (BV-10 KT Brown Type micropipette beveller; Sutter Instrument Co., Novato, CA, USA) using a programmable microinjector (Microdata Instruments, Plainfield, NJ, USA) as described.[52] Care was taken to avoid the lens during injection and if the lens was damaged, these mice were excluded from subsequent analysis. Local, intravitreal LPS injection is an effective route of administration to induce retinal inflammation as systemic application can result in transient inhibition of the ability of polymorphonuclear neutrophils (PMNs) to infiltrate into ocular tissue.[51]

Suspension Array Assay for Quantification of Cytokines/Chemokines

At 12 and 24 hours after LPS or PBS injection, mice were euthanized and retinas were carefully dissected under a stereo dissecting microscope (Zeiss Stemi DV4; Carl Zeiss Microscopy, Jena, Germany). Care was taken to remove vitreous humor from the inner retinal surface. Retinas were homogenized in PBS with proteinase inhibitors and centrifuged at 16,000 *g* to clarify the soluble fraction. Soluble fractions from individual retinas were analyzed for mouse IL-1β, IL-6, KC/CXCL1, MCP-1/CCL2, IL-10, IL-17, and TNFα on a custom-designed suspension array (Bio-Rad Life Science, Hercules, CA, USA) per manufacturer's instructions and as previously described.[53]

Quantification of Blood–Retinal Barrier Breakdown

Blood–retinal barrier permeability was assessed by a FITC-dextran assay as previously described.[23,54] Briefly, anesthetized mice were injected with 100 μL of FITC-dextran (4 kDa, 50 mg/mL; Sigma-Aldrich Corp.) into the circulation. After a 15-minute circulation time, 100 μL blood was collected, mice were perfused with 10 mL of PBS, retinas were collected, weighed, and FITC-dextran was extracted and filtered. For blood samples, plasma was isolated by centrifugation, and diluted. Fluorescence in plasma and retinal extracts was measured (excitation 485 nm/emission 538 nm) in a plate reader (BMG LabTech, Gmbh, Ortenberg, Germany) and the amount of FITC-dextran was calculated based on a standard curve generated from the injected FITC-dextran solution. Retinal autofluorescence was corrected using uninjected controls. Blood–retinal barrier breakdown was determined by the following formula, with results being presented as microliter plasma per gram of wet retina weight per hour:

$$\frac{\text{Retinal FITC} - \text{dextran}\,(\mu g)/\text{retinal weight}\,(g)}{\text{Plasma FITC} - \text{dextran concentration}\,(\mu g/\mu l)\cdot\text{circulation time}\,(h)} \quad (1)$$

Flow Cytometry

Flow cytometry was performed on retinal samples as described previously for neural tissues with minor modification.[55] Twenty-four hours after LPS or PBS injection, mice were perfused with PBS to remove nonadherent intravascular cells and retinas were homogenized with a Wheatley Dounce homogenizer (Thermo Fisher Scientific, Waltham, MA, USA) in RPMI 1640 and suspensions were passed through a 40-μm nylon cell strainer (Thermo Fisher Scientific). Samples were blocked with FcBlock anti-mouse CD16/32 (BD Biosciences, San Jose, CA, USA) followed by the addition of rat serum (Jackson ImmunoResearch Laboratories, West Grove, PA, USA). Surface markers were analyzed using PE-Cy5-conjugated anti-mouse CD45 (clone 30-F11; eBioscience, San Diego, CA, USA), PE-conjugated anti-mouse Ly-6G(Gr-1) (clone RB6-8C5; eBioscience), and FITC-conjugated anti-mouse F4/80 (clone BM8; eBioscience). Samples were washed three times with 1.0% BSA in PBS and single-cell suspensions were fixed overnight with 1% paraformaldehyde (PFA) and resuspended in 1% BSA in PBS for flow cytometry. Flow cytometry was performed on a Coulter Epics XL flow cytometer (Beckman Coulter, Brea, CA, USA). Events were gated by forward and side scatter, as well as by high expression of CD45 to distinguish infiltrating immune

Investigative Ophthalmology & Visual Science

cells ($CD45^{hi}$) from resident microglia ($CD45^{low}$). To determine leukocytes counts, we normalized to Countbright Absolute fluorescent counting beads (Life Technologies, Grand Island, NY, USA) and the absolute count of leukocytes was extrapolated from the ratio of the count of the gated population to the count of the counting beads present at a known concentration.

Retinal Leukostasis Assay

Twenty-four hours after intravitreal injections of LPS or PBS vehicle, leukostasis was assessed by a perfusion-based technique using FITC-conjugated Concanavalin A (FITC-ConA; Vector Laboratories, Burlingame, CA, USA) to label the adherent leukocytes and vascular endothelium as previously described with slight modifications.[56] Mice were deeply anesthetized and the chest cavity was fully open. After drainage was achieved from the right atrium, the mice were perfused with the following reagents in order, at a flow rate of approximately 9 to 10 mL/min: (1) PBS (0.1 mg/mL heparin) to remove blood and nonadherent leukocytes, (2) 2% PFA, (3) PBS, (4) 1% BSA in PBS, and (5) ConA (20 μg/mL) in 1% BSA-PBS. Each reagent was perfused over a 2-minute span (~20 mL). After perfusion, eyes were enucleated and retinas were carefully dissected and whole mounted for imaging on either an Olympus FV500 or 1200 confocal laser microscope (Olympus, Center Valley, PA, USA).

Histology, Immunohistochemistry, and Quantification of Extravascular Immune Cells

Localization of immune cells and retinal antigens was performed on paraffin-embedded retinal sections and on retinal whole-mounts as previously described with minor modification.[23,34] For retinal sections, eyes were removed from mice euthanized by CO_2 inhalation and whole globes were fixed with Prefer fixative (Anatech Ltd., Battle Creek, MI, USA) and processed for paraffin sectioning in the University of Oklahoma Health Sciences Center National Eye Institute (Bethesda, MD, USA)-supported imaging core. Five-micrometer sections through the optic nerve head were deparaffinized and stained with hematoxylin and eosin as previously described.[34] For immunolocalization of PMNs, deparaffinized sections were washed with PBS containing 0.1% Triton X-100 (PBST) and blocked with 10% normal horse serum in PBST. Sections were labeled with rat anti-Gr1 (eBioscience) and rabbit anti-GFAP (Dako, Carpinteria, CA, USA) and appropriate Alexa Fluor-conjugated secondaries (Life Technologies). Nuclei were counterstained with DAPI (Sigma-Aldrich Corp.).

Retinal whole-mounts were prepared as described[23] following fixation with 4% PFA. Retinas were permeabilized with 1% Triton X-100 in PBS (PBST), blocked with 10% normal horse serum in PBST and incubated overnight with rat anti-CD45 (BD Biosciences) and Alexa Fluor-488-conjugated secondary antibody. Retinal vasculature was counterstained with Alexa Fluor-594-conjugated isolectin B_4 from *Griffonia simplicifolia*. For localization of tight junction proteins, eyecups were fixed in 4% PFA with magnesium and calcium for a reduced fixation time of 15 minutes. Retinas were incubated with the following primary antibodies for 3 to 4 days at 4°C: rat anti-ZO-1 (1:50; EMD Millipore, Billerica, MA, USA), mouse anti-occludin (1:50; Invitrogen, Grand Island, NY, USA) and FITC-conjugated mouse anti-claudin-5 (1:100; Invitrogen). After extensively washing with 0.3% Triton X-100 in TBS, the retinas were incubated with appropriate fluorophore-conjugated secondary antibodies (1:500; Invitrogen; 1:200; Jackson ImmunoResearch) for 24 hours at 4°C. After extensively washing in 0.3% Triton X-100 in TBS, retinas were mounted ganglion cell layer up in glycerol: PBS (1:1, vol/vol). Whole mounts were imaged on an Olympus Fluoview 1200 confocal microscope with optical sections focused on the large retinal veins/venules in the superficial retina. The numbers of total and extravascular $CD45^{hi}$ immune cells were quantified by ImageJ software (http://imagej.nih.gov/ij/; provided in the public domain by the National Institutes of Health, Bethesda, MD, USA). For tight junction image analysis, images were imported and color channels split. After background subtraction, individual vessels were chosen as regions of interest for measurements. Repeat command was executed for all three channels and the values of mean intensity were collected for comparison.

Quantitative Real-Time PCR

Twenty-four hours after LPS or vehicle (PBS) injection, retinas were dissected and immediately snap frozen in liquid N_2. Total RNA was isolated using Aurum total RNA mini kit (Bio-Rad). One microgram of RNA was prepared for cDNA synthesis using iScript cDNA synthesis kit (Bio-Rad). The levels of *Tlr4* and inflammasome-related genes (*Nlrp1*, *Nlrp3*, and *Pycard*) and *Rpl19* (housekeeping gene) transcripts were measured by quantitative real-time PCR (qRT-PCR) using SYBR Green PCR mix (Bio-Rad) and the CFX96 real-time PCR detection system (Bio-Rad) following the manufacturer's instructions. Primers were designed to span intron-exon boundaries to avoid potential amplification of residual genomic DNA in RNA extraction. Relative quantities of individual transcript expression were calculated by the comparative Ct (threshold cycle) value method. Primer sequences and product sizes are summarized in Supplementary Table S1.

Western Blotting

Protein samples, SDS-PAGE, and Western blotting were performed as previously described [23] using the following antibodies and dilutions: rat anti–ZO-1 (1:1000; EMD Millipore); rabbit anti-occludin (1:500; Life Technologies); rabbit anti–claudin-5 (1:500; Life Technologies); rabbit anti–Cav-1 (1:3000; BD Biosciences); and mouse anti–β-actin (1:10,000; Abcam, Cambridge, MA, USA). Immunoreactivity was detected using species-appropriate horseradish peroxidase (HRP)-conjugated secondary antibodies (1:5000; GE Healthcare, Cleveland, OH, USA). Western blots were imaged and densitometric analyses performed using a Kodak In Vivo F-Pro imaging system (Carestream, Rochester, NY, USA).

Graphing and Statistical Analysis

Data were expressed as the mean ± SEM. Graphing and statistical analyses were performed using Prism5 software (GraphPad Software, La Jolla, CA, USA). For comparing two means, Student's *t*-test was used and for comparing more than two means, one-way ANOVA with the Newman-Keuls post hoc analysis was employed. *P* values less than 0.05 were considered statistically significant.

Results

Cav-1 Deficiency Blunts Innate Inflammatory Signaling

Caveolin-1 is dramatically upregulated in retinal inflammatory disease,[35] and Cav-1 has been found to regulate TLR4 signaling in pulmonary inflammation.[36,38,41] Furthermore, TLR4 contains a consensus Cav-1 binding motif within the Toll/IL-1 receptor (TIR) domain,[50] the intracellular domain that interacts with TLR adaptors. Therefore, we reasoned that Cav-1 might

Investigative Ophthalmology & Visual Science

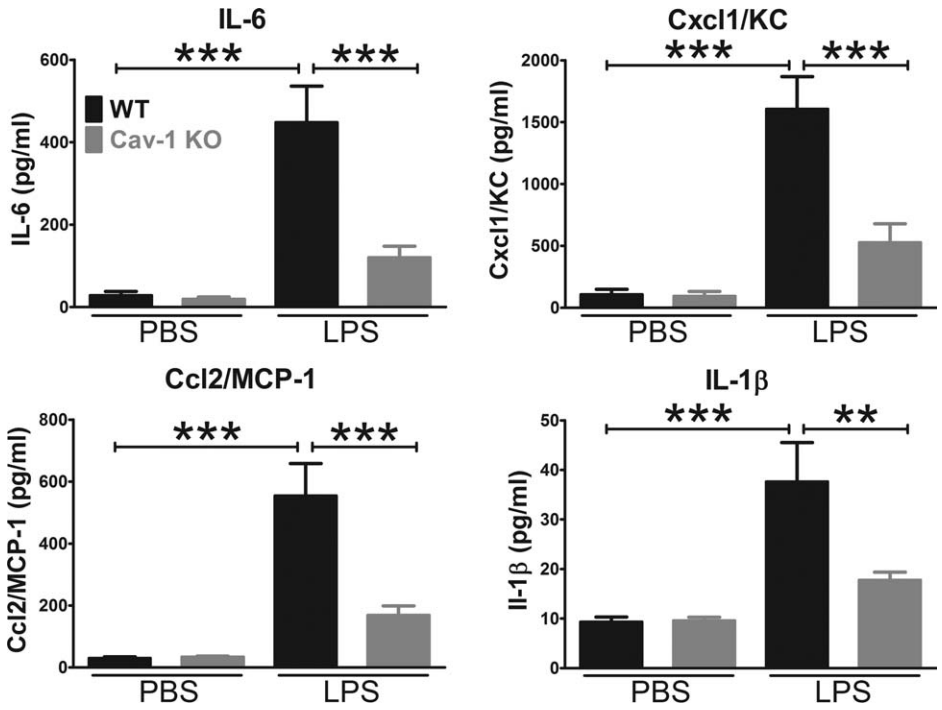

Figure 1. Caveolin-1 deficiency blunts LPS-induced innate inflammatory signaling. Endotoxin was intravitreally injected and retinas were collected 24 hours after inflammatory challenge and processed for multiplex protein suspension array analysis. Lipopolysaccharide challenge induced a characteristic NF-κB–driven inflammatory response in control (WT) mice compared with PBS-injected contralateral eyes. Caveolin-1 deficiency resulted in significant blunting of this inflammatory response ($n = 8$, mean ± SEM, $^{***}P < 0.001$, $^{**}P < 0.01$, ANOVA with Newman-Keuls post hoc test).

regulate innate immune signaling in the retina. To test this hypothesis, we applied the well-established endotoxin-induced uveitis model[51] to mice deficient in Cav-1 through intravitreal injection of the TLR4 ligand, LPS, and measured cytokine/chemokine levels in the retina after 24 hours. As shown in Figure 1, intravitreal injection of LPS induced the expected increase the protein levels of nuclear factor kappa-light chain-enhancer of activated B cells (nuclear factor [NF]-κB)-induced cytokine/chemokines (IL-6, Cxcl1/KC, Ccl2/MCP-1, and IL-1β) in WT control retinas. However, this response was significantly attenuated in Cav-1 null retinas. In addition to IL-6, Cxcl1/KC, Ccl2/MCP-1, and IL-1β, we also measured IL-17, TNFα, and the anti-inflammatory, IL-10 but these factors were not induced by LPS (Supplementary Fig. S1). In fact, IL-17 and IL-10 were significantly reduced 24 hours after LPS challenge in both WT and Cav-1 KO retinas. These results indicate that Cav-1 promotes inflammatory signaling mediated, most likely, by TLR4 and that Cav-1 deficiency suppresses inflammatory signaling.

To assess whether cytokine levels were different at an earlier time point, we repeated the multiplex protein array analysis at 12 hours post LPS challenge. As shown in Supplementary Figure S2, Cxcl1/KC, Ccl2/MCP-1, and IL-1β were also significantly dampened in LPS-challenged Cav-1 KO mice compared with WT controls. Surprisingly, IL-6 was not significantly blunted at this earlier time point and the reduction in Cxcl1/KC was not as dramatically blunted. This coupled with our 24 hour results may suggest that Cav-1 deficiency results in less prolonged cytokine responses or that there is a different cellular source for IL-6 at the earlier post challenge time.

In an effort to explain the reduced TLR4-mediated inflammatory signaling in Cav-1 deficient mice, we measured *Tlr4* expression levels by qRT-PCR. As shown in Supplementary Figure S3, we did not observe any significant differences in *Tlr4* expression levels with or without stimulation by LPS in Cav-1 KO or control retinas. If anything, there was a small but insignificant increase in *Tlr4* expression in LPS-treated Cav-1 KO retinas compared with controls. These results indicate that reduced *Tlr4* expression does not explain the dampened cytokine response in Cav-1–deficient retinas. Intravitreal LPS can increase intraocular levels of IL-1β.[57,58] As activation of the inflammasome is necessary to process IL-1β from pro- to active form it is possible that dampened IL-1β in Cav-1 KO retinas could result from inflammasome deficiency. However, we did not observe significant differences in expression of inflammasome components nucleotide-binding domain and leucine rich repeat (NLR) family, pyrin domain containing 3 (*Nlrp3*), *Nlrp1*, nor PYD and CARD domain containing (*Pycard*) mRNA (Supplementary Fig. S3). However, we do note a small decrease in basal expression of *Pycard* in Cav-1–deficient retinas but this did not reach statistical significance.

Cav-1 Deficiency Blunts Inflammation-Induced Blood–Retinal Barrier Breakdown

Our previous results indicated an important role of Cav-1 in maintaining the BRB.[23] However, as Cav-1 deficiency clearly suppressed retinal inflammatory signaling, we tested the impact of superimposing an inflammatory stimulus on BRB integrity. We intravitreally injected LPS as described and assessed BRB integrity 24 hours after inflammatory induction using a quantitative, FITC-dextran permeability assay.[23,54] As shown in Figure 2, inflammatory challenge resulted in a dramatic increase in BRB permeability in WT mice compared with the contralateral PBS-injected eye as has been previously reported.[59] To our surprise, Cav-1 deficiency significantly reduced BRB hyperpermeability induced by LPS challenge. Permeability in PBS-injected contralateral eyes of both WT and

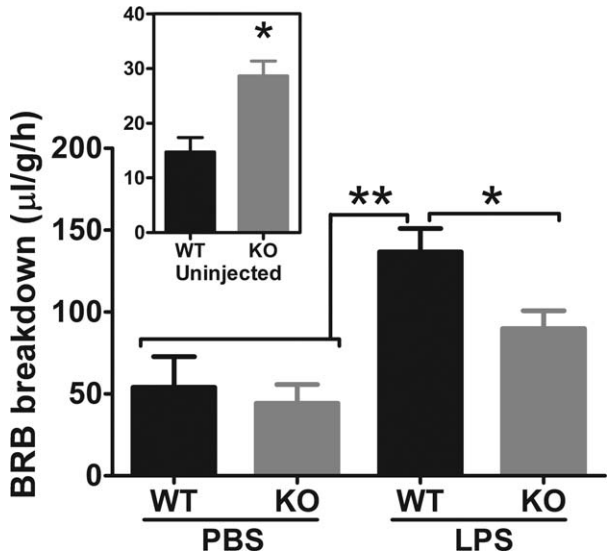

FIGURE 2. Caveolin-1 deficiency blunts LPS-induced BRB breakdown. Blood–retinal barrier integrity was assessed by FITC-dextran assay in mice challenged with LPS in one eye and PBS in the contralateral eye. Blood–retinal barrier breakdown was increased in naïve (uninjected) Cav-1 KO mice (*Inset*, $n = 4$, $^{*}P < 0.05$, unpaired *t*-test) but was significantly blunted in LPS challenged mice compared with WT controls ($n = 4$ WT and $n = 6$ KO; mean ± SEM, $^{**}P < 0.001$, $^{*}P < 0.05$, ANOVA with Newman-Kuels post hoc test).

Cav-1 KO mice was increased compared with naïve, uninjected mice (Fig. 2, inset) but was not different between genotypes. Increased basal permeability in naïve Cav-1 KO mice was similar to that previously reported[23] indicating that while basal permeability is elevated, the much more profound inflammation-induced permeability was paradoxically suppressed. In fact, when normalized to control levels of permeability in naïve mice, this represented a 10.2-fold increase in WT and only a 2.8-fold increase in Cav-1 KO mice. The lack of difference in permeability in PBS-injected eyes and the relative increase over naïve mice suggests an influence of either the vehicle injection itself or of a systemic effect of contralateral LPS injection. However, this effect did not manifest in increased cytokine levels in PBS-injected WT control eyes (Fig. 1). Finally, these results indicate that the mechanism by which Cav-1 expression reduces basal BRB integrity is different from the one that promotes permeability under inflammatory conditions.

Given the dampened inflammation-induced BRB permeability in Cav-1 KO mice, we examined the levels of tight junction proteins, ZO-1, occludin, and claudin-5 in whole-retinal lysates by Western blot analysis. As shown in Supplementary Figure S4, we observed no significant differences in the levels of these proteins between genotypes although we found a trend toward reduced ZO-1 levels following LPS challenge in both genotypes. As the LPS effect on tight junction integrity might be localized to specific vessels (i.e., in locations with leukostasis), we followed up our Western blot analysis with imaging analyses (as described in reference 23) on individual retinal vessels in whole mounts from $n = 3$ retinas per treatment/genotype (Supplementary Fig. S5). As shown, we observed few changes in tight junction protein localization/immunoreactivity in either genotype with or without LPS challenge. Claudin-5 immunoreactivity was modestly reduced in LPS-treated retinas from both genotypes. Occludin immunoreactivity was increased in LPS-challenged, Cav-1 KO vessels compared with similarly challenged control retinas, which could represent reduced ability to internalize occludin following inflammatory insult as has been previously reported.[60] Consistent with our immunoblot analysis (Supplementary Fig. S4), we found that LPS challenge resulted in reduced levels of ZO-1 immunoreactivity independent of genotype.

Histology of Endotoxin-Induced Uveitis in Cav-1 KO Eyes

Given the reduced inflammatory signaling we predicted that the inflammation induced by LPS injection would also be reduced in Cav-1 KO mice. To test this notion, we initially carried out a histologic analysis of ocular sections from Cav-1 KO and WT mouse eyes injected with LPS or vehicle. As shown in Figure 3, robust PMN infiltrate was observed in the anterior chamber and vitreous of both genotypes 24 hours after LPS challenge. We noted regions of the Cav-1 KO retina that contained numerous immune cell infiltration and retinal dysmorphia, including disruption of the RPE, retinal detachment, and folding indicative of edema (Fig. 3B). These results suggested a qualitatively similar immune cell infiltration anteriorly in both genotypes and a more pronounced posterior inflammatory response in Cav-1 KO compared with WT retinas. To confirm that this cellular infiltrate was immune cell-derived, we stained retinal sections with Gr1 to label PMNs and inflammatory monocytes in this experimental model. As shown in Supplementary Figure S6, qualitatively similar numbers of Gr1+ cells were observed in the vitreous of LPS-challenged eyes from both genotypes. In dysmorphic regions

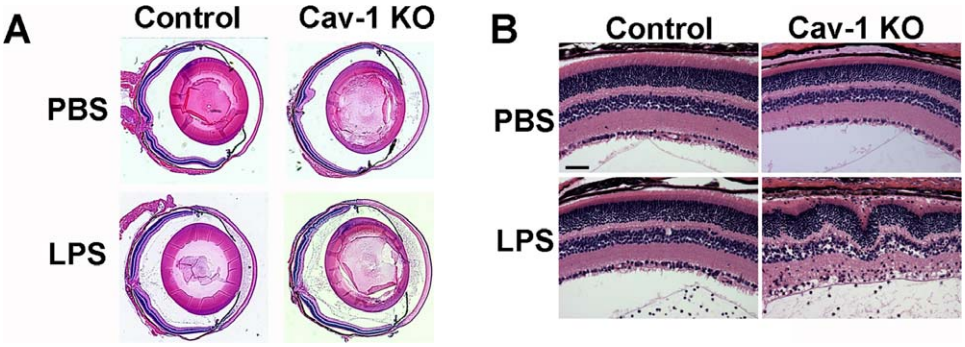

FIGURE 3. Histologic analysis of LPS-induced inflammation in Cav-1 deficient eyes. (**A**) Representative sections of whole globes (**A**) and regions of retinas (**B**) in LPS- and PBS-injected Cav-1 deficient and control mouse eyes. Similar anterior segment and vitreous infiltrates were observed but regions of Cav-1 KO retinas displayed more inflammatory disruption than controls. *Scale bar*: 50 µm.

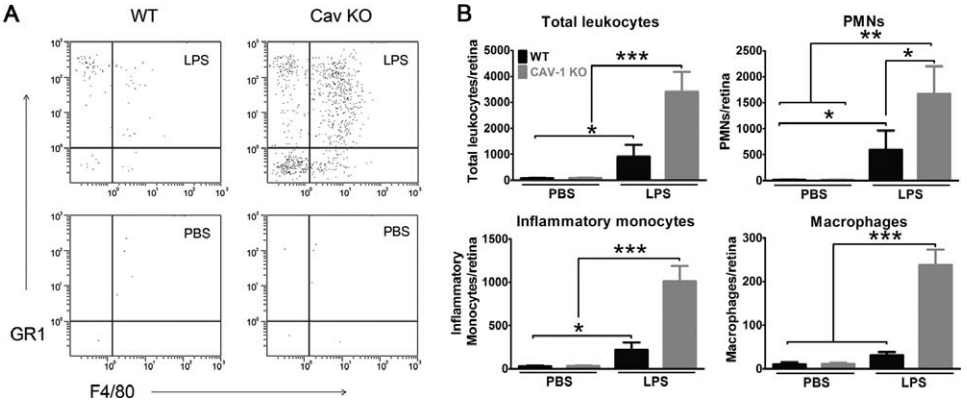

Figure 4. Caveolin-1 deficiency results in increased immune cell recruitment in response to acute inflammatory challenge. Intravitreal LPS challenge induced a significant increase in immune cell numbers in retinas from Cav-1 KO mice compared with controls. Cells that expressed high levels of CD45 ($CD45^{hi}$, total leukocytes) and PMNs (F4/80–; Gr1+), inflammatory monocytes (F4/80+; Gr1+), and macrophages (F4/80+; Gr1-) were quantified. (**A**) Representative flow cytometry dot plots for a Cav-1 KO and control mouse. (**B**) Quantification of immune cell populations (results from $n = 15$ samples from three combined experiments; mean ± SEM, $^{***}P < 0.001$, $^{**}P < 0.01$, $^{*}P < 0.05$, ANOVA with Newman-Keuls post hoc test).

of the Cav-1 KO retina, the cellular infiltrate was also confirmed to be Gr1+. These results suggest that Gr1+ cell infiltration is actually more pronounced in Cav-1 KO retinas even though LPS-driven chemoattractants are reduced.

Cav-1 Deficiency Results in Increased Immune Cell Numbers in LPS-Challenged Retinas

To quantify the observed qualitative increase in retinal inflammation, we carried out flow cytometry to quantify retinal inflammation in Cav-1 KO retinas following LPS challenge. We used an established flow cytometry protocol gated on total leukocytes ($CD45^{hi}$) and sorted by the expression of F4/80 and Gr1 (Fig. 4A).[53] Using this protocol, we could distinguish between PMNs (F4/80–;Gr1+), inflammatory monocytes (F4/80+;Gr1+), and macrophages (F4/80+; Gr1–). These combined cell types constituted the majority (86% in Cav-1 KO and 93% in control) of total $CD45^{hi}$ cells at 24 hours post LPS challenge. As suggested by our histologic analyses, we observed a significantly greater number of immune cells in LPS-challenged Cav-1 KO compared with WT retinas (Figs. 4A, 4B). The majority of detected immune cells at this time point were PMNs (49% in Cav-1 KO and 66% in control) followed by inflammatory monocytes (30% in Cav-1 KO and 24% in control) and macrophages (7% in Cav-1 KO and 3% in control). The low numbers of immune cells in contralateral PBS-injected eyes indicated that the PBS vehicle did not induce immune cell adhesion/recruitment. These results clearly suggested a conundrum with an increase in immune cell recruitment/infiltration in LPS-challenged Cav-1 KO compared with WT retinas even though recruiting cytokine/chemokine expression was suppressed (Fig. 1, Supplementary Fig. S2).

Cav-1 Deficient Immune Cells are Competent to Extravasate

Our results suggest a disconnection between the expression of select leukocyte chemoattractants and the number of recruited immune cells residing in Cav-1–deficient retinas. We next determined whether Cav-1–deficient leukocytes were capable of extravasation by comparing the number of extravasated immune cells versus those within vessels in retinal flatmounts from LPS- and vehicle-challenged eyes. In these experiments, mice were not perfused intravenously prior to tissue harvesting and fixation. As leukocyte extravasation usually occurs in retinal veins, we focused our analysis on large veins in the superficial retina. Intravitreal LPS challenge induced a significant increase in the ratio of extravasated/total CD45-positive immune cells in both genotypes compared with the contralateral PBS-injected eye (Fig. 5). We did not observe significant differences in this ratio between genotypes suggesting that the Cav-1 KO immune cells are capable of extravasation. In agreement with our flow cytometry analysis, we observed more CD45-positive cells in LPS-challenged Cav-1 KO compared with LPS-challenged WT retinas (Figs. 5C, 5D, 5G, 5H). However, to our surprise, we observed a significant increase in the total number of immune cells in Cav-1 deficient, PBS-injected contralateral eyes compared to PBS-injected controls (30 ± 3 vs. 4 ± 2; Cav-1 KO versus control) with the majority of these cells localized within vessel lumen (29 ± 3 vs. 4 ± 2; Cav-1 KO versus control). When we examined adherent leukocytes by a well-established leukostasis assay that involves the imaging of concanavalin-labeled intraluminal immune cells adhering after intravenous perfusion,[56] we found increased leukostasis in LPS-challenged Cav-1 KO retinas compared with similarly challenged WT retinas (Fig. 6). However, dramatic differences in adherent leukocytes were not found in retinas from contralateral PBS-injected eyes suggesting that the vascular endothelium of PBS-injected contralateral eyes did not promote leukocyte adhesion in either genotype. Collectively, these results suggest either that Cav-1 KO mice have more circulating immune cells under naïve conditions or that the contralateral LPS injection induced systemic immune cell activation differentially.

To determine whether Cav-1 KO mice have more circulating immune cells basally, we examined blood samples from naïve Cav-1 KO and WT mice by flow cytometry. As shown in Figure 7, we found a significant increase in leukocytes and significantly elevated monocyte counts in peripheral blood from naïve Cav-1 KO mice not injected with LPS compared with WT control mice. In agreement with this result, a recent paper describing the importance of Cav-1 in monocyte to macrophage differentiation observed a similar increase in circulating monocytes in global Cav-1 KO mice.[61] Thus, these results could, in part, explain the paradoxically increased numbers of immune cells in Cav-1 retinas even given the reduced chemoattractant expression that results from Cav-1 deficiency.

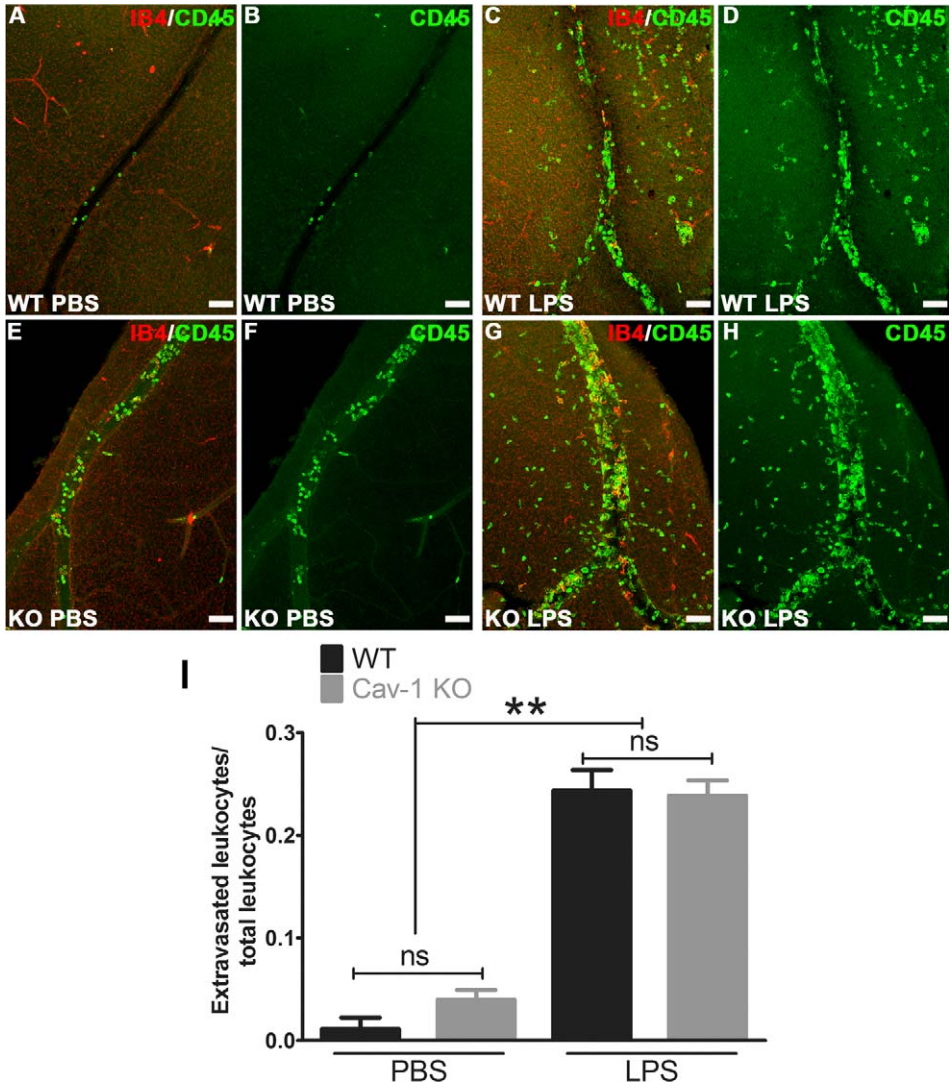

Figure 5. Ratio of extravascular/total CD45-positive immune cells was not different between LPS-challenged Cav-1 KO and WT retinas. Retinal flatmounts were stained with CD45 (*green*) and isolectin-B4 (IB4, *red*). (**A–H**) Representative confocal stacks of whole mounts from WT and Cav-1 KO retinas focused on retinal veins in the superficial layer. (**I**) Results of quantification of ratios of extravascular/total immune cells ($n = 3$, mean ± SEM, $^{**}P < 0.01$, $^{*}P < 0.05$, ANOVA with Newman-Keuls post hoc test). *Scale bar*: 50 μm. ns = not significant.

Discussion

Herein, we define a novel role for Cav-1 in the regulation of acute retinal inflammation. These results in combination with other studies describing profound increases in Cav-1 expression in retinal inflammatory diseases such as autoimmune uveitis[35] and in animal models of diabetic retinopathy[4,19] suggest that Cav-1 may be a clinically-relevant regulator of retinal inflammation. Furthermore, recent findings associating the CAV1 and CAV2 genes with POAG,[62–65] another disease with a significant inflammatory component but poorly understood disease mechanism, suggest the possibility of a link to this ocular disease. Our results are paradoxical in that they demonstrate that Cav-1 deficiency attenuates proinflammatory cytokine/chemokine signaling and inflammatory BRB breakdown while at the same time resulting in increased immune cell recruitment/infiltration. However, this paradox may be explained, at least in part, by differential Cav-1 functions in cell-specific contexts during acute inflammatory challenge and merit further studies to define the mechanisms behind this complex response. A second explanation that is possible but less likely is that cytokine signaling is enhanced in Cav-1 KO retinas at earlier time points after inflammatory challenge. We note that IL-6 levels, which are dampened at 24 hours were not reduced at 12 hours post challenge, although they were certainly not elevated in Cav-1 KO at this earlier time. Furthermore, other cytokines were significantly blunted even at 12 hours. However, we cannot exclude the possibility that an earlier signal is recruiting leukocytes in Cav-1 KO mice. Given the multifaceted roles of Cav-1 in such relevant cellular processes as vascular barrier homeostasis,[23,66] transendothelial[67–69] (and trans-RPE[70]) immune cell trafficking, inflammatory signaling,[36,38,41,44,48,50,71] and systemic immune cell functions,[61,72] we propose that our results in globally Cav-1 deficient animals could be explained by complex interactions between local retinal signaling, BRB dysfunction, and systemic immune dysregulation.

Consistent with results observed in inflammatory lung disease,[38,41,44] we found that Cav-1 expression promotes inflammatory cytokine/chemokine expression in response to LPS challenge. Furthermore, similar promotion of inflammatory signaling by Cav-1 in models of bacterial and viral infection

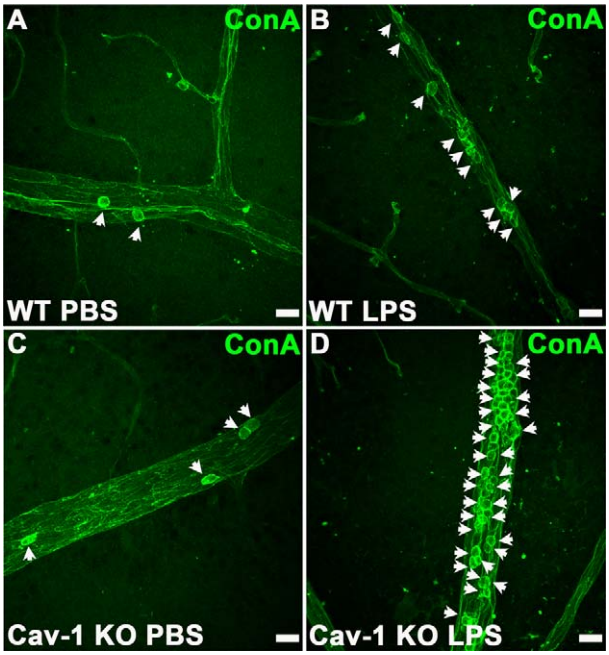

FIGURE 6. Increased leukostasis in LPS-challenged Cav-1 KO retinas. Leukostasis was assessed by perfusion of FITC-ConA. Images show representative regions of retinal veins. *Scale bar*, 20 μm.

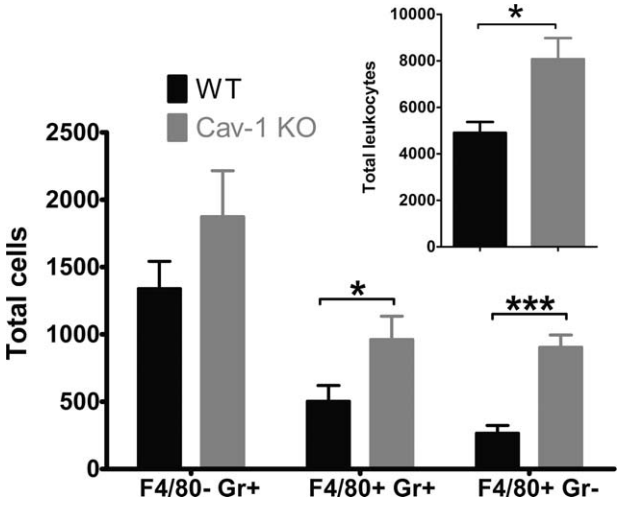

FIGURE 7. Caveolin-1 deficiency alone (without inflammatory challenge) results in increased circulating immune cells. Flow cytometry was performed on peripheral blood as described. Significant increases in total immune cells and in monocytes were observed in Cav-1 KO mice compared with WT controls ($n = 10$ WT and $n = 11$ Cav-1 KO samples, mean ± SEM, $^{***}P < 0.001$, $^{*}P < 0.05$, unpaired *t*-test).

in the cornea has been recently reported.[43,73] In the retina, the mechanism of this signaling suppression and the cell type responsible for our findings are as yet undetermined. However, our results suggest that a cell type that expresses high levels of proinflammatory cytokines when activated (e.g., microglia, infiltrating immune cells, vascular endothelium) or abundant retina-intrinsic cells (e.g., Müller glia or RPE) could be a local source of the inflammatory cytokine/chemokine production. Müller glial cells, in particular, have been found to be major innate sensors for TLR agonists in the retina.[74] We and others have observed abundant Cav-1 expression in Müller glia and retinal vascular endothelium,[14–16,19–21,23,33,34] more modest expression in RPE and mural cells,[17,18,23] and little to no detectable expression in retinal microglia (data not shown). Caveolin-1 expression has also been identified in PMNs[72] and monocytes/macrophages.[61] Thus, differential effects of Cav-1 on inflammatory signaling in cell-specific sources remains a possible explanation for our finding of suppressed inflammatory signaling but enhanced inflammatory cell recruitment.

Our previous[23] and current results (Fig. 2, inset) have demonstrated that Cav-1 deficiency alone renders the BRB hyperpermeable under basal conditions. Although cytokine/chemokine levels were significantly blunted in Cav-1 deficient retinas (Fig. 1), we did observe increased levels over vehicle-treated eyes although this increase did not reach statistical significance. This suggests the possibility that although inflammatory signaling is reduced, the blunted signal may still be sufficient to recruit and promote infiltration of leukocytes to inflamed Cav-1–deficient retinas with compromised barrier integrity. However, we note that the much more profound increase in BRB permeability induced by LPS was significantly blunted in Cav-1 KO retinas suggesting that the increased basal BRB permeability and the LPS-induced breakdown act through distinct mechanisms. The most logical explanation for the suppression of inflammatory BRB breakdown in Cav-1 KO retinas is reduced production of permeability-inducing proinflammatory cytokine expression resulting from Cav-1 deficiency. For example, it has been shown that MCP-1/CCL2 can exert direct effects on endothelial barrier integrity in the central nervous system by reducing the levels of tight junction proteins occludin and ZO-1.[75] Another possibility for the paradoxical effect of Cav-1 on basal and inflammatory BRB breakdown is that the increased fluorescent dextran flux under inflammatory conditions occurs through the outer RPE barrier. We have defined that basal BRB hyperpermeability occurs at local sites in the retinal venous system and not through the RPE.[23] Further, in preliminary studies on RPE-specific Cav-1 KO mice, we have not observed basal BRB breakdown (unpublished observation). However, the effect of inflammation on RPE-specific Cav-1 KO mice has not yet been tested.

As already indicated, an additional question is why more leukocyte recruitment is observed in Cav-1 KO retinas in the context of reduced cytokine/chemokine signaling. Our results (Fig. 6) and others have suggested that global Cav-1 deficiency results in systemic immune dysfunction including a reduced ability for PMNs to adhere/extravasate and a reduction in monocyte/macrophage differentiation.[61,72] We observed significant increases in circulating peripheral immune cells as a consequence of Cav-1 deficiency in the absence of inflammatory challenge. We also observed significant intravascular immune cells in PBS-injected eyes from mice with contralateral LPS challenge (Figs. 5E, 5F). These results suggest that in the absence of Cav-1 the immune system is primed for inflammatory response. The significant increase in circulating monocytes observed by flow cytometry (Fig. 6) are in agreement with results recently describing the importance of Cav-1 in monocyte to macrophage differentiation where similarly elevated blood monocytes were reported in Cav-1 KO mice.[61] However, we found that the ratio of extravascular to total immune cells was similar in Cav-1 KO and WT mice even in the context of increased total immune cells suggesting that Cav-1 deficient immune cells were competent to extravasate. These results contrast with others suggesting that Cav-1 deficiency results in impaired recruitment and extravasation of PMNs.[72] We cannot explain this discrepancy but hypothesize that Cav-1 KO retinal vasculature is more permeable to leukocytes. We should note that Cav-1 has been identified as a component of transendothelial[67] and trans-RPE[70] pores that can promote

Investigative Ophthalmology & Visual Science

immune cell transmigration but whether Cav-1 is necessary for pore formation remains ambiguous. However, our results suggest that Cav-1–deficient leukocytes are capable of accessing the generally tight retinal barrier.

In conclusion, the current findings support a novel and complex role in the retinal response to an acute inflammatory stimulus. Although our results do not define the response to chronic inflammation, they clearly suggest the possibility that Cav-1 is involved in a variety of retinal/ocular inflammatory conditions.

Acknowledgments

The authors thank the expert assistance of Mark Dittmar, manager of the Dean McGee Eye Institute vivarium, the National Eye Institute core-supported imaging core module for expert histologic preparations, and finally, Holly Rosenzweig at the Oregon Health & Science University for valuable advice on the establishment of the EIU model.

Supported by National Institutes of Health (Bethesda, MD, United States) Grants: EY019494 (MHE), EY012985, EY024140 (MCC), EY021238 (DJJC), EY022071 (NM), National Eye Institute (Bethesda, MD, United States) core Grant P30EY021725; Sybil B. Harrington Special Scholar Award for Macular Degeneration Research from Research to Prevent Blindness, Inc. (New York, NY, United States), an unrestricted Grant from Research to Prevent Blindness, Inc. (New York, NY, United States), and a Natural Science Foundation of China Grant 81300800 (XL; Beijing, China).

Disclosure: **X. Li**, None; **X. Gu**, None; **T.M. Boyce**, None; **M. Zheng**, None; **A.M. Reagan**, None; **H. Qi**, None; **N. Mandal**, None; **A.W. Cohen**, None; **M.C. Callegan**, None; **D.J.J. Carr**, None; **M.H. Elliott**, None

References

1. Streilein JW. Ocular immune privilege: the eye takes a dim but practical view of immunity and inflammation. *J Leukoc Biol*. 2003;74:179–185.
2. Caspi RR. A look at autoimmunity and inflammation in the eye. *J Clin Invest*. 2010;120:3073–3083.
3. Strauss O. The retinal pigment epithelium in visual function. *Physiol Rev*. 2005;85:845–881.
4. Klaassen I, Van Noorden CJ, Schlingemann RO. Molecular basis of the inner blood-retinal barrier and its breakdown in diabetic macular edema and other pathological conditions. *Prog Retin Eye Res*. 2013;34:19–48.
5. Streilein JW, Ma N, Wenkel H, Ng TF, Zamiri P. Immunobiology and privilege of neuronal retina and pigment epithelium transplants. *Vision Res*. 2002;42:487–495.
6. Wenkel H, Streilein JW. Evidence that retinal pigment epithelium functions as an immune-privileged tissue. *Invest Ophthalmol Vis Sci*. 2000;41:3467–3473.
7. Sugita S, Horie S, Yamada Y, Mochizuki M. Inhibition of B-cell activation by retinal pigment epithelium. *Invest Ophthalmol Vis Sci*. 2010;51:5783–5788.
8. Forrester JV. Bowman lecture on the role of inflammation in degenerative disease of the eye. *Eye (Lond)*. 2013;27:340–352.
9. Nickells RW, Howell GR, Soto I, John SW. Under pressure: cellular and molecular responses during glaucoma, a common neurodegeneration with axonopathy. *Annu Rev Neurosci*. 2012;35:153–179.
10. Kleinman ME, Baffi JZ, Ambati J. The multifactorial nature of retinal vascular disease. *Ophthalmologica*. 2010;224(suppl 1):16–24.
11. Antonetti DA, Klein R, Gardner TW. Diabetic retinopathy. *N Engl J Med*. 2012;366:1227–1239.
12. Parton RG, del Pozo MA. Caveolae as plasma membrane sensors, protectors and organizers. *Nat Rev Mol Cell Biol*. 2013;14:98–112.
13. Cohen AW, Hnasko R, Schubert W, Lisanti MP. Role of caveolae and caveolins in health and disease. *Physiol Rev*. 2004;84:1341–1379.
14. Gu X, Reagan A, Yen A, Bhatti F, Cohen AW, Elliott MH. Spatial and temporal localization of caveolin-1 protein in the developing retina. *Adv Exp Med Biol*. 2014;801:15–21.
15. Roesch K, Jadhav AP, Trimarchi JM, et al. The transcriptome of retinal Müller glial cells. *J Comp Neurol*. 2008;509:225–238.
16. Nelson BR, Ueki Y, Reardon S, et al. Genome-wide analysis of Müller glial differentiation reveals a requirement for Notch signaling in postmitotic cells to maintain the glial fate. *PLoS One*. 2011;6:e22817.
17. Mora RC, Bonilha VL, Shin BC, et al. Bipolar assembly of caveolae in retinal pigment epithelium. *Am J Physiol Cell Physiol*. 2006;290:C832–C843.
18. Bridges CC, El-Sherbeny A, Roon P, et al. A comparison of caveolae and caveolin-1 to folate receptor alpha in retina and retinal pigment epithelium. *Histochem J*. 2001;33:149–158.
19. Klaassen I, Hughes JM, Vogels IM, Schalkwijk CG, Van Noorden CJ, Schlingemann RO. Altered expression of genes related to blood-retina barrier disruption in streptozotocin-induced diabetes. *Exp Eye Res*. 2009;89:4–15.
20. Stitt AW, Burke GA, Chen F, McMullen CB, Vlassara H. Advanced glycation end-product receptor interactions on microvascular cells occur within caveolin-rich membrane domains. *FASEB J*. 2000;14:2390–2392.
21. Feng Y, Venema VJ, Venema RC, Tsai N, Behzadian MA, Caldwell RB. VEGF-induced permeability increase is mediated by caveolae. *Invest Ophthalmol Vis Sci*. 1999;40:157–167.
22. Hofman P, Blaauwgeers HG, Tolentino MJ, et al. VEGF-A induced hyperpermeability of blood-retinal barrier endothelium in vivo is predominantly associated with pinocytotic vesicular transport and not with formation of fenestrations. Vascular endothelial growth factor-A. *Curr Eye Res*. 2000;21:637–645.
23. Gu X, Fliesler SJ, Zhao YY, Stallcup WB, Cohen AW, Elliott MH. Loss of caveolin-1 causes blood-retinal barrier breakdown, venous enlargement, and mural cell alteration. *Am J Pathol*. 2014;184:541–555.
24. Caldwell RB, Slapnick SM. Freeze-fracture and lanthanum studies of the retinal microvasculature in diabetic rats. *Invest Ophthalmol Vis Sci*. 1992;33:1610–1619.
25. Raviola G, Butler JM. Unidirectional vesicular transport mechanism in retinal vessels. *Invest Ophthalmol Vis Sci*. 1983;24:1465–1474.
26. Gardiner TA, Archer DB. Does unidirectional vesicular transport occur in retinal vessels? *Br J Ophthalmol*. 1986;70:249–254.
27. Elliott MH, Nash ZA, Takemori N, Fliesler SJ, McClellan ME, Naash MI. Differential distribution of proteins and lipids in detergent-resistant and detergent-soluble domains in rod outer segment plasma membranes and disks. *J Neurochem*. 2008;104:336–352.
28. Kachi S, Yamazaki A, Usukura J. Localization of caveolin-1 in photoreceptor synaptic ribbons. *Invest Ophthalmol Vis Sci*. 2001;42:850–852.
29. Boesze-Battaglia K, Dispoto J, Kahoe MA. Association of a photoreceptor-specific tetraspanin protein, ROM-1, with triton X-100-resistant membrane rafts from rod outer segment disk membranes. *J Biol Chem*. 2002;277:41843–41849.
30. Elliott MH, Fliesler SJ, Ghalayini AJ. Cholesterol-dependent association of caveolin-1 with the transducin alpha subunit in

bovine photoreceptor rod outer segments: disruption by cyclodextrin and guanosine 5′-O-(3-thiotriphosphate). *Biochemistry*. 2003;42:7892–7903.

31. Berta AI, Boesze-Battaglia K, Magyar A, Szel A, Kiss AL. Localization of caveolin-1 and c-src in mature and differentiating photoreceptors: raft proteins co-distribute with rhodopsin during development. *J Mol Histol*. 2011;42:523–533.
32. Chen W, Jump DB, Esselman WJ, Busik JV. Inhibition of cytokine signaling in human retinal endothelial cells through modification of caveolae/lipid rafts by docosahexaenoic acid. *Invest Ophthalmol Vis Sci*. 2007;48:18–26.
33. Opreanu M, Tikhonenko M, Bozack S, et al. The unconventional role of acid sphingomyelinase in regulation of retinal microangiopathy in diabetic human and animal models. *Diabetes*. 2011;60:2370–2378.
34. Li X, McClellan ME, Tanito M, et al. Loss of caveolin-1 impairs retinal function due to disturbance of subretinal microenvironment. *J Biol Chem*. 2012;287:16424–16434.
35. Hauck SM, Dietter J, Kramer RL, et al. Deciphering membrane-associated molecular processes in target tissue of autoimmune uveitis by label-free quantitative mass spectrometry. *Mol Cell Proteomics*. 2010;9:2292–2305.
36. Jin Y, Lee SJ, Minshall RD, Choi AM. Caveolin-1: a critical regulator of lung injury. *Am J Physiol Lung Cell Mol Physiol*. 2011;300:L151–L160.
37. Chidlow JH Jr, Sessa WC. Caveolae, caveolins, and cavins: complex control of cellular signalling and inflammation. *Cardiovasc Res*. 2010;86:219–225.
38. Mirza MK, Yuan J, Gao XP, et al. Caveolin-1 deficiency dampens Toll-like receptor 4 signaling through eNOS activation. *Am J Pathol*. 2010;176:2344–2351.
39. Walton KA, Cole AL, Yeh M, et al. Specific phospholipid oxidation products inhibit ligand activation of toll-like receptors 4 and 2. *Arterioscler Thromb Vasc Biol*. 2003;23:1197–1203.
40. Tsai TH, Chen SF, Huang TY, et al. Impaired Cd14 and Cd36 expression, bacterial clearance, and Toll-like receptor 4-Myd88 signaling in caveolin-1-deleted macrophages and mice. *Shock*. 2011;35:92–99.
41. Jiao H, Zhang Y, Yan Z, et al. Caveolin-1 Tyr14 phosphorylation induces interaction with TLR4 in endothelial cells and mediates MyD88-dependent signaling and sepsis-induced lung inflammation. *J Immunol*. 2013;191:6191–6199.
42. Medina FA, Cohen AW, de Almeida CJ, et al. Immune dysfunction in caveolin-1 null mice following infection with Trypanosoma cruzi (Tulahuen strain). *Microbes Infect*. 2007;9:325–333.
43. Reidy T, Rittenberg A, Dwyer M, D'Ortona S, Pier G, Gadjeva M. Homotrimeric macrophage migration inhibitory factor (MIF) drives inflammatory responses in the corneal epithelium by promoting caveolin-rich platform assembly in response to infection. *J Biol Chem*. 2013;288:8269–8278.
44. Garrean S, Gao XP, Brovkovych V, et al. Caveolin-1 regulates NF-kappaB activation and lung inflammatory response to sepsis induced by lipopolysaccharide. *J Immunol*. 2006;177:4853–4860.
45. Feng H, Guo L, Song Z, et al. Caveolin-1 protects against sepsis by modulating inflammatory response, alleviating bacterial burden, and suppressing thymocyte apoptosis. *J Biol Chem*. 2010;285:25154–25160.
46. Zhang PX, Murray TS, Villella VR, et al. Reduced caveolin-1 promotes hyperinflammation due to abnormal heme oxygenase-1 localization in lipopolysaccharide-challenged macrophages with dysfunctional cystic fibrosis transmembrane conductance regulator. *J Immunol*. 2013;190:5196–5206.
47. Gadjeva M, Paradis-Bleau C, Priebe GP, Fichorova R, Pier GB. Caveolin-1 modifies the immunity to Pseudomonas aeruginosa. *J Immunol*. 2010;184:296–302.
48. Wang XM, Kim HP, Song R, Choi AM. Caveolin-1 confers antiinflammatory effects in murine macrophages via the MKK3/p38 MAPK pathway. *Am J Respir Cell Mol Biol*. 2006;34:434–442.
49. Medina FA, de Almeida CJ, Dew E, et al. Caveolin-1-deficient mice show defects in innate immunity and inflammatory immune response during Salmonella enterica serovar Typhimurium infection. *Infect Immun*. 2006;74:6665–6674.
50. Wang XM, Kim HP, Nakahira K, Ryter SW, Choi AM. The heme oxygenase-1/carbon monoxide pathway suppresses TLR4 signaling by regulating the interaction of TLR4 with caveolin-1. *J Immunol*. 2009;182:3809–3818.
51. Rosenbaum JT, Woods A, Kezic J, Planck SR, Rosenzweig HL. Contrasting ocular effects of local versus systemic endotoxin. *Invest Ophthalmol Vis Sci*. 2011;52:6472–6477.
52. Ramadan RT, Ramirez R, Novosad BD, Callegan MC. Acute inflammation and loss of retinal architecture and function during experimental Bacillus endophthalmitis. *Curr Eye Res*. 2006;31:955–965.
53. Conrady CD, Zheng M, van Rooijen N, et al. Microglia and a functional type I IFN pathway are required to counter HSV-1-driven brain lateral ventricle enlargement and encephalitis. *J Immunol*. 2013;190:2807–2817.
54. Ishida S, Usui T, Yamashiro K, et al. VEGF164 is proinflammatory in the diabetic retina. *Invest Ophthalmol Vis Sci*. 2003;44:2155–2162.
55. Wuest TR, Carr DJ. Dysregulation of CXCR3 signaling due to CXCL10 deficiency impairs the antiviral response to herpes simplex virus 1 infection. *J Immunol*. 2008;181:7985–7993.
56. Joussen AM, Murata T, Tsujikawa A, Kirchhof B, Bursell SE, Adamis AP. Leukocyte-mediated endothelial cell injury and death in the diabetic retina. *Am J Pathol*. 2001;158:147–152.
57. Kezic J, Taylor S, Gupta S, Planck SR, Rosenzweig HL, Rosenbaum JT. Endotoxin-induced uveitis is primarily dependent on radiation-resistant cells and on MyD88 but not TRIF. *J Leukoc Biol*. 2011;90:305–311.
58. Rosenzweig HL, Woods A, Clowers JS, Planck SR, Rosenbaum JT. The NLRP3 inflammasome is active but not essential in endotoxin-induced uveitis. *Inflamm Res*. 2012;61:225–231.
59. Trichonas G, Manola A, Morizane Y, et al. A novel nonradioactive method to evaluate vascular barrier breakdown and leakage. *Invest Ophthalmol Vis Sci*. 2010;51:1677–1682.
60. Stamatovic SM, Keep RF, Wang MM, Jankovic I, Andjelkovic AV. Caveolae-mediated internalization of occludin and claudin-5 during CCL2-induced tight junction remodeling in brain endothelial cells. *J Biol Chem*. 2009;284:19053–19066.
61. Fu Y, Moore XL, Lee MK, et al. Caveolin-1 plays a critical role in the differentiation of monocytes into macrophages. *Arterioscler Thromb Vasc Biol*. 2012;32:e117–e125.
62. Loomis SJ, Kang JH, Weinreb RN, et al. Association of CAV1/CAV2 genomic variants with primary open-angle glaucoma overall and by gender and pattern of visual field loss. *Ophthalmology*. 2014;121:508–516.
63. Thorleifsson G, Walters GB, Hewitt AW, et al. Common variants near CAV1 and CAV2 are associated with primary open-angle glaucoma. *Nat Genet*. 2010;42:906–909.
64. Wiggs JL, Kang JH, Yaspan BL, et al. Common variants near CAV1 and CAV2 are associated with primary open-angle glaucoma in Caucasians from the USA. *Hum Mol Genet*. 2011;20:4707–4713.

65. Kang JH, Loomis SJ, Yaspan BL, et al. Vascular tone pathway polymorphisms in relation to primary open-angle glaucoma. *Eye (Lond)*. 2014;28:662–671.
66. Song L, Ge S, Pachter JS. Caveolin-1 regulates expression of junction-associated proteins in brain microvascular endothelial cells. *Blood*. 2007;109:1515–1523.
67. Carman CV, Springer TA. A transmigratory cup in leukocyte diapedesis both through individual vascular endothelial cells and between them. *J Cell Biol*. 2004;167:377–388.
68. Engel D, Beckers L, Wijnands E, et al. Caveolin-1 deficiency decreases atherosclerosis by hampering leukocyte influx into the arterial wall and generating a regulatory T-cell response. *FASEB J*. 2011;25:3838–3848.
69. Marmon S, Hinchey J, Oh P, et al. Caveolin-1 expression determines the route of neutrophil extravasation through skin microvasculature. *Am J Pathol*. 2009;174:684–692.
70. Omri S, Behar-Cohen F, de Kozak Y, et al. Microglia/macrophages migrate through retinal epithelium barrier by a transcellular route in diabetic retinopathy: role of PKCzeta in the Goto Kakizaki rat model. *Am J Pathol*. 2011;179:942–953.
71. Cai L, Yi F, Dai Z, et al. Loss of caveolin-1 and adiponectin induces severe inflammatory lung injury following LPS challenge through excessive oxidative/nitrative stress. *Am J Physiol Lung Cell Mol Physiol*. 2014;306:L566–L73.
72. Hu G, Ye RD, Dinauer MC, Malik AB, Minshall RD. Neutrophil caveolin-1 expression contributes to mechanism of lung inflammation and injury. *Am J Physiol Lung Cell Mol Physiol*. 2008;294:L178–L186.
73. Yousuf MA, Zhou X, Mukherjee S, et al. Caveolin-1 associated adenovirus entry into human corneal cells. *PLoS One*. 2013;8:e77462.
74. Kumar A, Shamsuddin N. Retinal Müller glia initiate innate response to infectious stimuli via toll-like receptor signaling. *PLoS One*. 2012;7:e29830.
75. Song L, Pachter JS. Monocyte chemoattractant protein-1 alters expression of tight junction-associated proteins in brain microvascular endothelial cells. *Microvasc Res*. 2004;67:78–89.

Investigative Ophthalmology & Visual Science